APPLICATIONS OF GEOSAT ALTIMETER DATA IN THE NORTH-EAST PACIFIC

J. F. R. Gower, and S. Tabata,
Institute of Ocean Sciences, P.O. Box 6000, Sidney, BC, V8L 4B2, Canada

Tel: (604) 356-6558, Fax: (604) 356-6479, Telex: 049-7281

ABSTRACT

The Geosat altimeter has successfully mapped sea surface height, ice, waves and winds during the 5 years of its life (1984-1989). We present two examples of the use of this data in the north-east Pacific. Consistent sea surface height anomalies with space scales of order 100-300km, are observed at 17 day intervals. Anomaly amplitudes are in the range 10 to 30 cm, with anomaly displacement velocities of about 1 cm/s. These altimetry results are compared with the more precise, but less frequent data from ship hydrographic and CTD measurements. Examples are also shown of wave-height maps derived from Geosat data. The spatial coverage pattern from a single satellite is insufficient to follow the pattern of waveheight growth and decay induced by the global surface wind field, but gives valuable statistical data on the long term average wave climate.

1 GEOSAT ALTIMETER DATA

A satellite altimeter measures the travel time of pulses emitted vertically downwards, and reflected back to the satellite by an area of the earth's surface typically a few kilometers across. Accurate knowledge of the satellite's position and of the pulses' propagation speed, allows measurement of the absolute height of the earth's surface. Over the oceans, the mean flatness of the sea surface on kilometer scales, and the symmetry of height offsets introduced by surface waves, allows a mean range to be determined with a precision of a few centimeters.

Such a precision gives important oceanographic data on ocean circulation and on smaller scale motions, since the geostrophic balance of these water movements on a rotating earth requires changes in the mean ocean surface height. These height variations are in the range 10 to 30cm for mesoscale eddies, and up to 100cm at the edges of intense western boundary currents. Horizontal scale of the height changes are of the order of 100km. Oceanic applications of satellite altimeter sea surface height data have been demonstrated by Cheney et al. (1983), Fu and Chelton (1985) and Tai et al. (1989).

The US Navy Geosat satellite was designed to provide classified information on the shape of the geoid. This has not been made available to the non-military research community. After completion of these measurements, the satellite orbit was altered to duplicate that of the Seasat mission from which similar data had already been made available in 1978. After November 1986, Geosat was held to within 1km of this nominal orbit and provided a sequence of global altimetry data which has been widely distributed. Some results from this mission were recently reported in a special journal issue introduced by Douglas and Cheney (1990).

This is the so-called Exact Repeat Mission (ERM) which began in November 1986, in which Geosat repeated its orbit pattern every 17.05 days. In this period, 244 satellite orbits covered an oblique grid with an equator crossing separation of 164km. This coverage pattern is defined by ascending node longitudes $1.05^{o}E + 360n/244$ for n = 1 to 244, orbit inclination of 108.04^{o} and an orbital period of 6037.55s.

2 OBSERVATIONS IN THE N.E. PACIFIC

The present study area is shown in Figure 1. Eddies were tracked in the two areas outlined by rectangles. Waveheights were studied in the full area 0 to $60^{o}N$, 90 to $180^{o}W$. For the eddy tracking use was made of ascending orbits which crossed this area with a mean spacing of about 90km as shown. These correspond to n = 141 to 173 in the formula for ascending node longitudes given above. Similar descending orbits also crossed this area approximately orthogonally to those shown. However, much of the data from descending orbits were unusable due to attitude instability of the satellite after crossing arctic Canada, and information from them is not considered here.

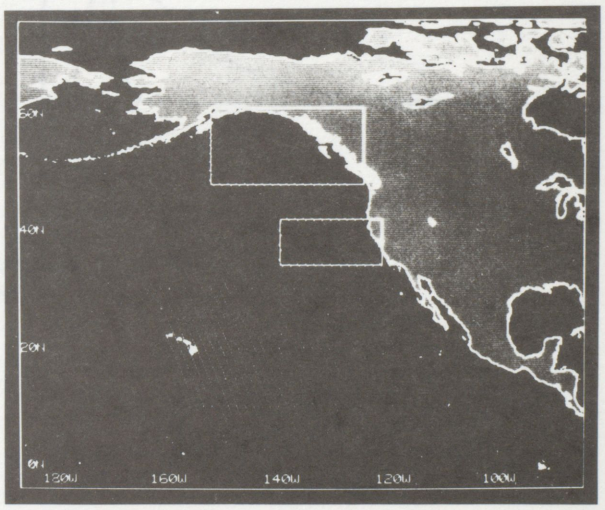

Figure 1. Map of the study area showing North America and the Hawaiian islands, the positions of Geosat ascending orbit tracks for n = 141 to 173 and rectangles outlining areas where eddies were tracked, west of California and in the Gulf of Alaska.

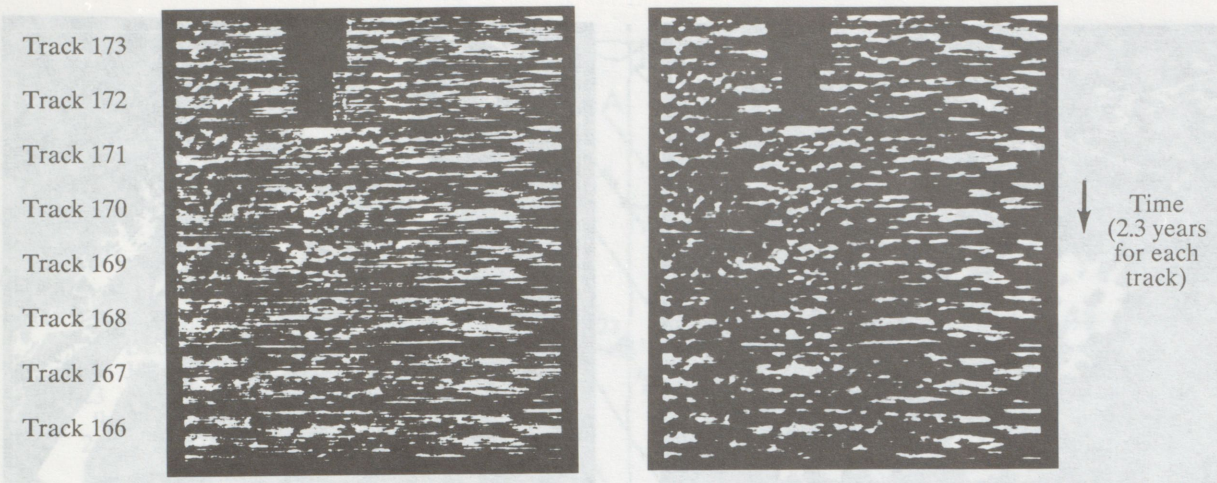

Figure 2. Grey scale time sequence plots of anomaly heights deduced from Geosat data. Heights are coded as image brightnesses for a range of ± 30cm about a mean value. Each rectangle contains the height anomaly data for 48 consecutive satellite cycles along one track from latitude 60°N to 0°N. Rectangles correspond to tracks for n = 173 (top, whose centre section lies over land) to 166 (bottom). Figure 2a (left) shows the unedited data. Figure 2b (right) shows the data after editing and smoothing.

Copies of tapes of the Geosat global data set were received from NOAA in the USA, via MEDS in Ottawa, typically 6 months after data collection. One 6250 bpi tape covers two 17 day cycles. Corrections listed on the tapes for variations in geoid height, solid earth and ocean tides, water vapour and atmospheric pressure (propagation and inverse barometer corrections), ionosphere electron content and satellite attitude, were applied to the altimetry data.

The major error remaining is due to inaccurate knowledge of the satellite's absolute vertical position. This can amount to several meters, but is slowly varying over a spatial scale of several thousand kilometers, since most of the error occurs at a spatial frequency of one cycle per orbit. The error for each orbit track was compensated in the present study by subtracting the best fit second order polynomial function of along-track distance from the observed surface heights. The correction was computed separately for the data in each satellite pass, using only data over deep water for which coverage extended over at least 80% of the latitude range 0° to 60°N.

Inaccuracy of the geoid heights listed on the Geosat data tapes is significant at the space scales (<500km) being studied here and prevents measurement of absolute ocean surface heights. We therefore compute height anomalies as the difference between the corrected heights, and the two year mean heights, along each track. A constant height anomaly in a fixed position will therefore be removed from the data when the mean observed height is subtracted. This will not affect the detection of moving anomalies, but should be born in mind when interpreting the data presented below.

Figure 2 shows the height anomalies computed in this way from Geosat data for 48 17 day cycles from November 1986 to February 1989. The height anomalies along each track are plotted along horizontal lines, coded as grey scale variations from black (about 30cm low) to white (about 30cm high), relative to a mean level shown as a neutral grey. Each rectangle consists of the 48 lines of observations, repeated at 17 day intervals, for one of eight passes whose tracks are plotted in Figure 1. The 48 lines are plotted one beneath the other and aligned vertically by latitude from 60°N at the left-hand end down to the equator at the right. The eight rectangles correspond to the eight right-most passes of those plotted in Figure 1. Gaps occur in the top two where these tracks cross the land-mass of North America.

Missed passes (20 out of 384 shown here) and about 2% of the data which were manually deleted, have been linearly interpolated. The data were then smoothed by convolving the numbers plotted in Figure 2 with a 3 by 3 filter matrix. This smoothing filter is graded to 60% at the edges and 40% at the corners. Since it is applied to samples separated by 20km along track, and by 17 day intervals in time, the effective smoothing (full width to half height of the filter) is over about 56 consecutive kilometers along track and about 2.8 intervals or 48 days.

The data in Figure 2 cover a time period of 2.3 years. Height variations with an annual period are visible on the left end of each track corresponding to positions close to the Alaska/Aleutian Island coast, and also at latitudes south of about 15°N. These larger scale phenomena have an amplitude of about 20cm. They may be artifacts of the corrections applied to the Geosat data. For the northern areas the tidal model is suspected. In the tropics the propagation delay due to the high water vapour content may not be correctly compensated. These features are not discussed further here.

In the Gulf of Alaska, the data clearly show positive height anomalies with coherence scales of order 150km (along the tracks shown) in space, and 3 months (about 5 repeat cycles or 85 days) in time (Gower, 1989a). These small-scale anomalies are more intense closer to the Alaska/BC coast (n = 171-173) than in passes further offshore, and are also concentrated to the left (north-west) ends of the tracks, implying less eddy activity further south in the Gulf of Alaska. In the top two tracks the southern Gulf of Alaska is dominated by larger scale features with an annual cycle.

Further south, between 40°N and 30°N the data again show increased eddy activity, and reduced activity between 30N and 15°N. South of 15°N the eddies are masked by the annual cycle.

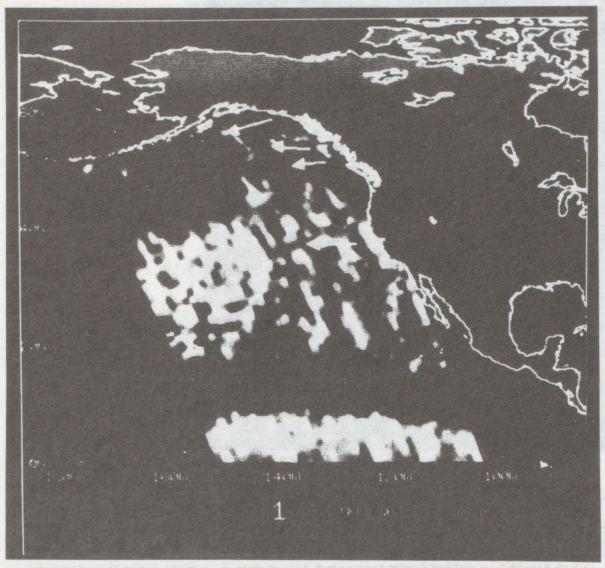

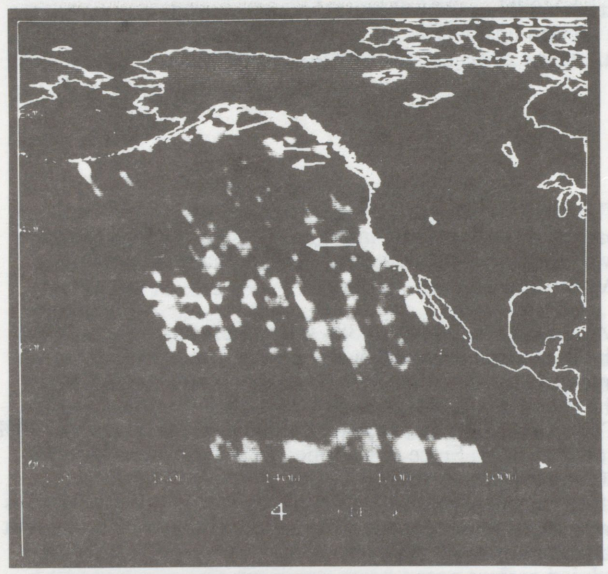

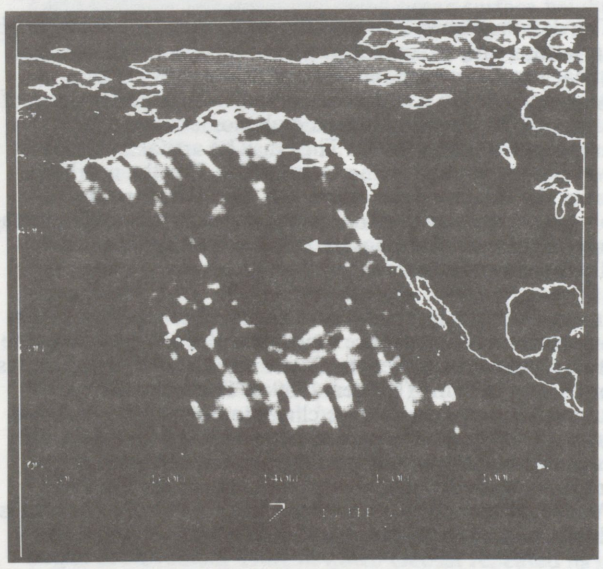

Figure 3. Grey scale images of anomaly heights in the north-east Pacific constructed from the data shown in Figure 2 and from 25 other tracks, for the cycles 1 (top, mean date, 16 Nov 1986), 4 (centre, 23 Jan 1987) and 7 (bottom, 26 Feb 1987).

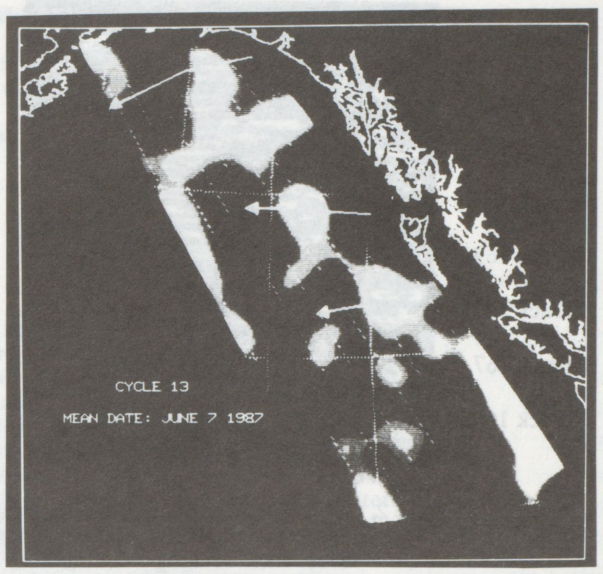

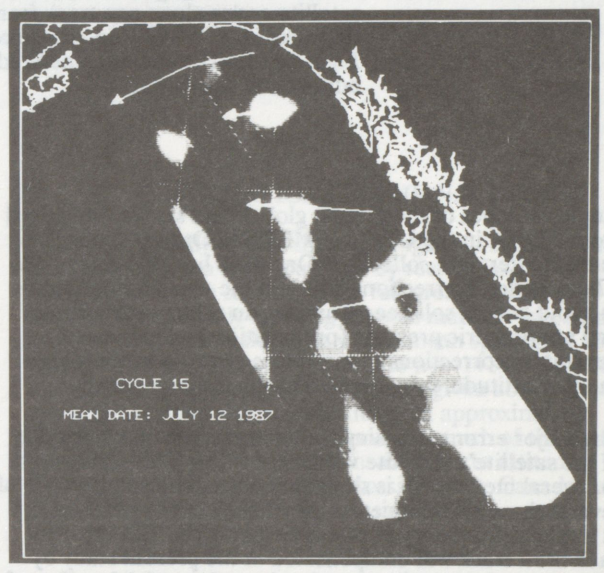

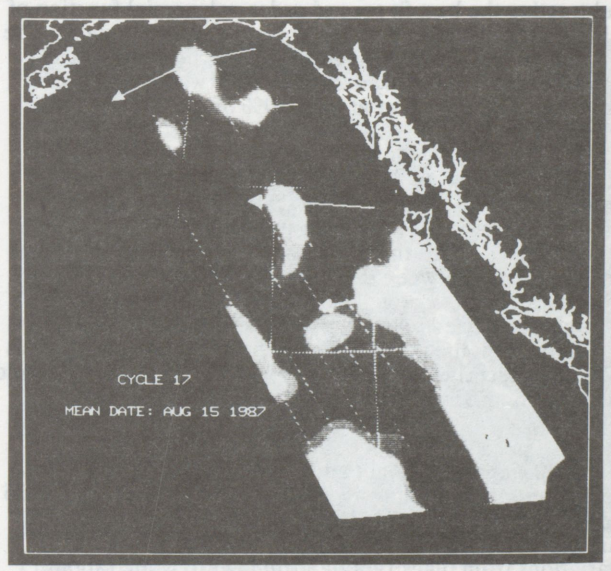

Figure 4. Grey scale images of anomaly heights in the Gulf of Alaska, constructed from the data shown in Figure 2 for cycle 13 (top, mean date, 8 June 1987), 15 (centre, 12 July 1987) and 17 (bottom, 15 August 1987).

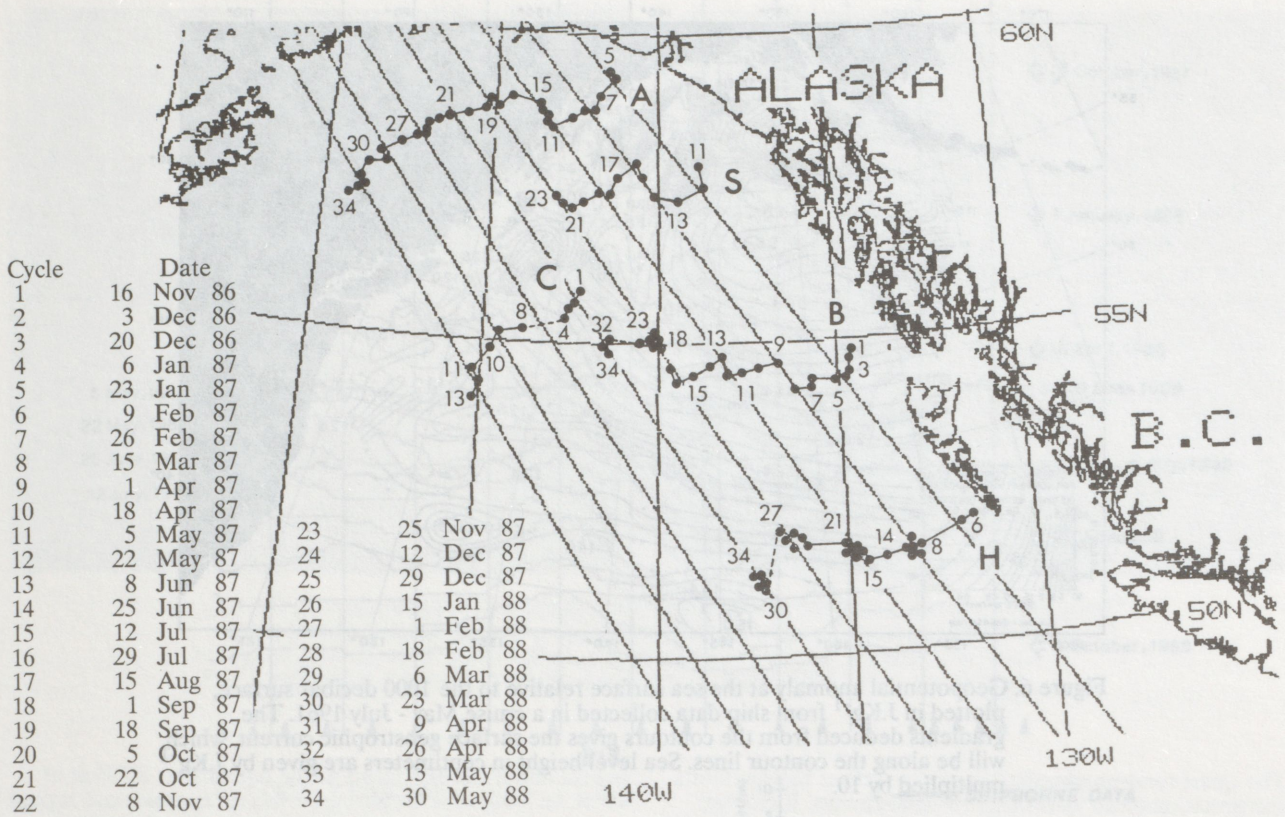

Cycle	Date			
1	16 Nov 86			
2	3 Dec 86			
3	20 Dec 86			
4	6 Jan 87			
5	23 Jan 87			
6	9 Feb 87			
7	26 Feb 87			
8	15 Mar 87			
9	1 Apr 87			
10	18 Apr 87			
11	5 May 87	23	25 Nov 87	
12	22 May 87	24	12 Dec 87	
13	8 Jun 87	25	29 Dec 87	
14	25 Jun 87	26	15 Jan 88	
15	12 Jul 87	27	1 Feb 88	
16	29 Jul 87	28	18 Feb 88	
17	15 Aug 87	29	6 Mar 88	
18	1 Sep 87	30	23 Mar 88	
19	18 Sep 87	31	9 Apr 88	
20	5 Oct 87	32	26 Apr 88	
21	22 Oct 87	33	13 May 88	
22	8 Nov 87	34	30 May 88	

Figure 5. Tracks of mean positions of height anomalies S, H, A, B and C, deduced from the image sequence of which Figure 3 is a part. Numbers indicate 17 day cycles whose mean dates are listed in the table at the left. Dashed lines indicate periods where a feature was not detectable.

3 EDDY DISTRIBUTION AND MOVEMENT

In Figures 3 and 4 interpolated height anomaly data for single 17 day periods are shown as grey scale images for different mean dates. The brightness scale is similar to that used in Figure 2. Data is interpolated between tracks using a gaussian weighted average with an e-folding distance of 60km as described by Gower (1989b). This distance was chosen as being the minimum needed to smoothly fill between tracks.

Figure 3 shows height anomalies in the north-east Pacific near the start of the Geosat ERM. The most striking, consistently observed height anomaly is indicated by the white arrow off the coast of California. This is a negative height anomaly (cyclonic eddy), moving westwards at about 2.5 cm/s over the period November 1986 to August 1987 from 126^{o} 20'W to 133^{o} 20'W at a latitude of 37^{o}N. (Mean speed over 273 days = 2.51 cm/s towards 268^{o}). A list of positions for this eddy is given in Table 1.

Arrows in the Gulf of Alaska indicate eddy motion there, shown on a larger scale in Figure 4. This Figure shows the height anomalies during cycles 13, 15 and 17, corresponding to mean dates June 7, July 12 and August 15 1987. Several anticyclonic eddy-like features (positive height anomalies) are evident, especially in the north-west half of the study area, and a westward movement can be seen in most cases. Mesoscale features are less evident in the region to the south-east, which is dominated by larger scale anomalies with an annual period, as noted above.

The data on the tracks plotted in Figure 4 (n = 166 to 173) are collected on days 13, 16, 2, 5, 8, 11, 14 and 1 respectively of the 17 day cycle. Displacements of the order of the track separation, occurring within this time could therefore be aliased on these plots. This would affect features with speeds greater than about 10cm/s. Slower moving features should be adequately sampled in time.

Figure 5 (from Gower, 1989b) shows a plot of the mean centroid positions of eddies identified from the data sequence of repeat cycles of Geosat data, covering November 1986 to May 1988. Mean positions and velocities are listed in Table 2. Those shown represent the main features that formed between cycles 1 and 20. Some eddies that formed later, whose tracks would have overlapped those shown, are omitted.

The eddy "S" is identified with the Sitka eddy previously reported in ship observations by Tabata (1982). The name "Haida" has been suggested for eddy "H". Other eddies are here labeled "A", "B" and "C".

The positions in Figure 5 appear to cluster on the satellite tracks, suggesting that the eddies are under-sampled by the satellite tracks, that is, that the width of a typical height anomaly is less than the track separation. In this case attempts to track peaks in a noisy background will tend to give locations nearly centered on a track.

Table 1 lists the results of eddy tracking in the Gulf of Alaska. Speeds are deduced from positions selected to reduce the effect of the clustering noted above. They are mostly in the range 1.0 to 1.4 cm/s, with headings between 240 and 280^{o} (through east from north), that is, westwards. Major differences from these mean values occur at the end of the data sequence (B 34 and H 34) or at the edge of the spatial coverage (C 13). Mean and standard deviations for all the values shown are 1.3 $\pm$ 0.4 cm/s in speed, and 252^{o} $\pm$ 28^{o} in direction.

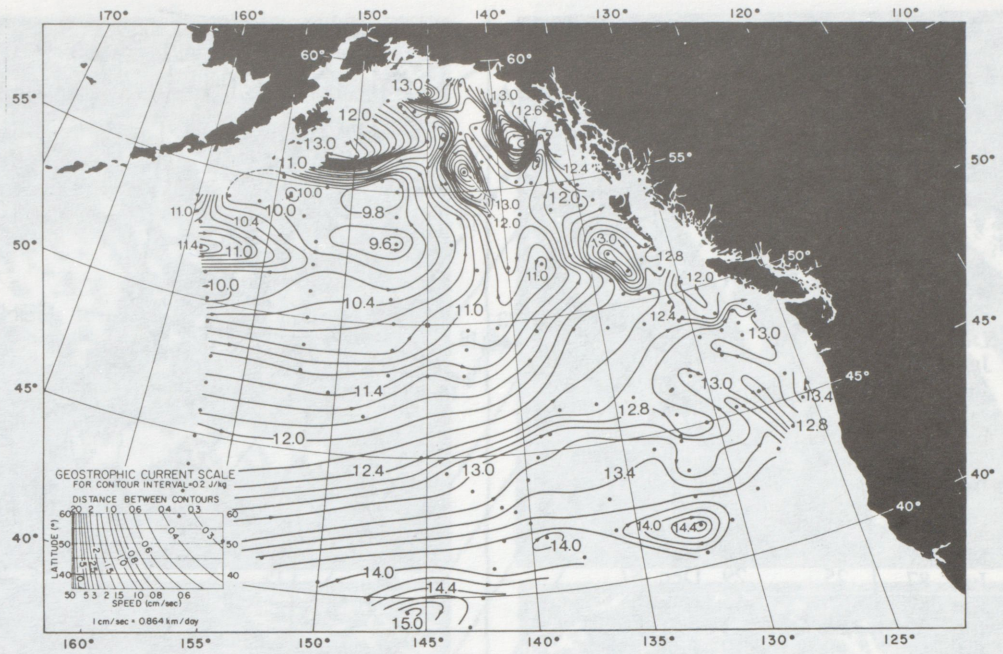

Figure 6. Geopotential anomaly at the sea surface relative to the 1000 decibar surface, plotted in $J.Kg^{-1}$ from ship data collected in a cruise May - July 1961. The gradients deduced from the contours gives the surface geostrophic current, which will be along the contour lines. Sea level height in centimeters are given by $J.Kg^{-1}$ multiplied by 10.

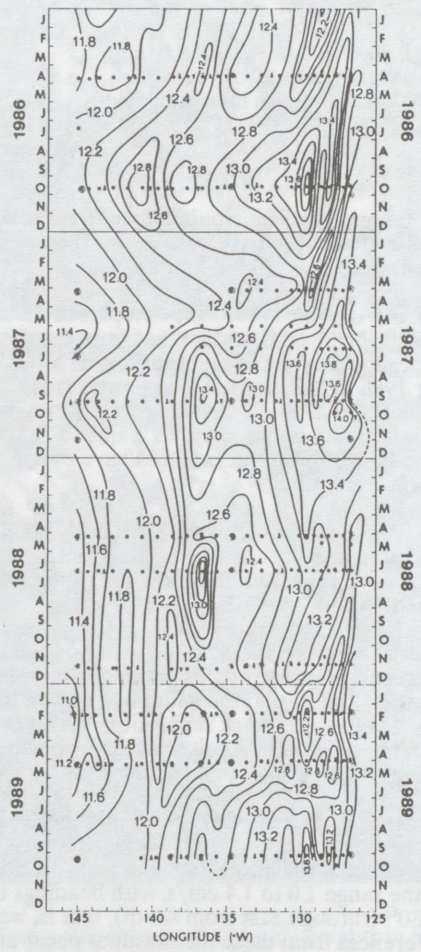

Figure 7. Geopotential anomaly at the sea surface relative to the 1000 decibar surface, plotted in $J.Kg^{-1}$ from cruises along line P in the years 1986-1989. Data for May 1988 and June/July 1988 are plotted in Figure 8.

These speeds and direction of movement agree with predictions for baroclinic Rossby waves and with a correlation of time series measurements along line P (White and Tabata, 1987). The magnitudes and distribution of the anomalies shown here compare well with the available ship observations, as discussed below.

4 COMPARISON WITH SHIP DATA

Previous studies of the height anomalies in this study area have been reported by Tabata (1982) who showed a series of maps of geopotential anomaly relative to 1000m deduced from hydrographic (bottle cast) station data measured on US/Canada ship cruises between 1956 and 1962. Stations covered an irregular grid with a spacing of 100 - 200km, concentrating on the area under the satellite tracks in Figure 1, but extending over the whole area shown. Typical cruise duration was about 30 days, but individual features tended to be covered in a period of a few days.

Figure 6 shows contours of geopotential anomaly at the sea surface relative to 1000 decibars (about 1000m), interpolated from stations occupied in the June 1961 cruise. They equivalent heights have similar magnitude and distribution to those in Figure 4, though the satellite data show more structure. The shape of the sea surface deduced from the ship measurements is clearly affected by the positions of ship stations. The largest height anomaly corresponds to the most active eddy reported by Tabata (1982). This appeared in about 50% of observations at a position off Sitka, Alaska, centered near 57°N, 138°W, and with a diameter of 200-300km. The other major height anomalies in the ship data (Figure 6) appear 300Km west-southwest of the "Sitka" eddy, further northwest close to the Alaska coast, and about 100km west-southwest of Cape St James (the southern point of the Queen Charlotte Islands),. Similar features also appear in Figure 4.

The satellite data show that an eddy is often present at the "Sitka" location, but that after forming at this location the eddies tend to move off to the west with a velocity of 1-2cm/s. An eddy is present in the generation area for cycles

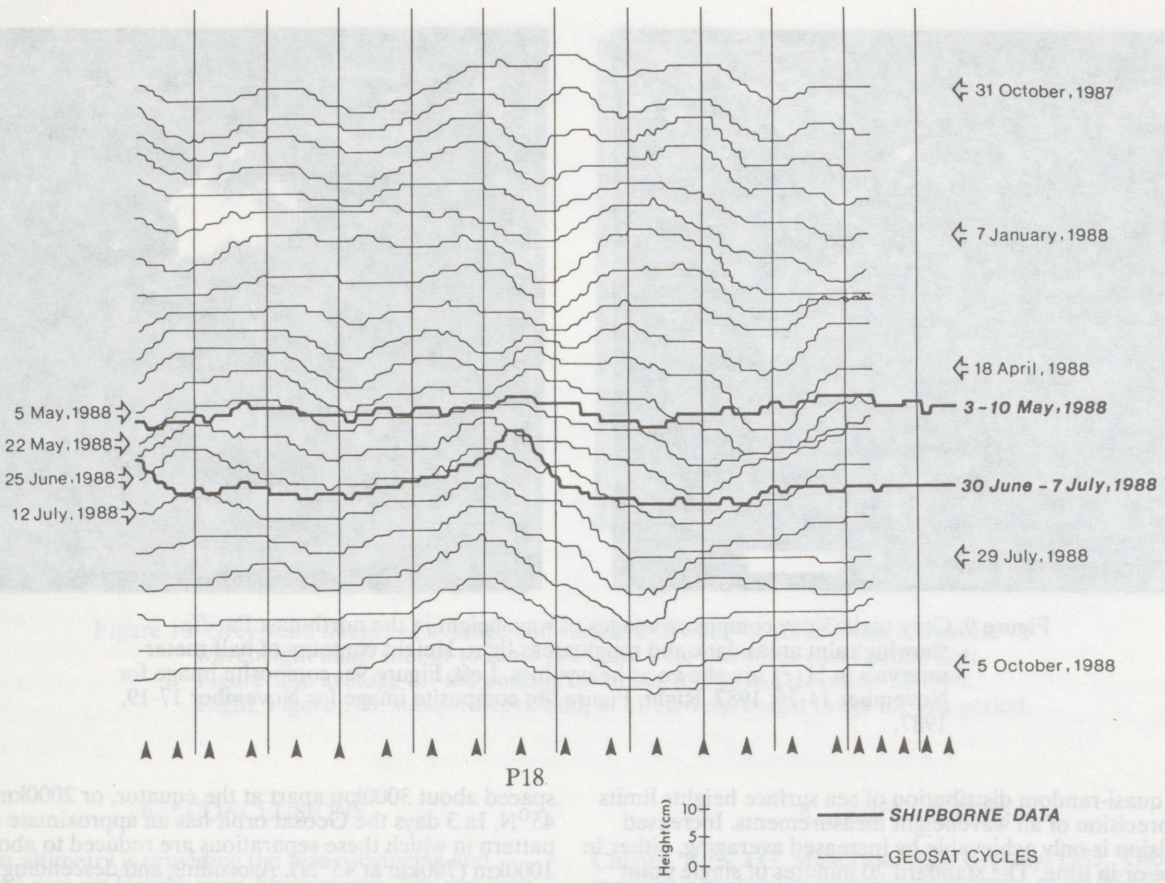

Figure 8. Cruise data on height anomalies compared with the sequence of satellite data extending from October 1987 to October 1988. The cruise data (heavy lines) for May and June/July 1988 are plotted over the corresponding satellite data. Measurements were taken at locations indicated by the vertical arrow-heads. The satellite data (faint lines) have been interpolated from measurements along satellite tracks that cross line P at the positions of the vertical lines.

11 to 16, before moving westwards, as shown in Figure 4. An eddy (not shown in Figure 5) later formed near the same location in cycle 29 and moved northwestwards for the remainder of the data sequence.

During the time of the Geosat ERM, the only place where hydrographic data were collected repeatedly in the Gulf of Alaska was along line P. This extends from the coast at the southern end on Vancouver Island out to the site of Ocean Station Papa (50^{o}N, 145^{o}W). A few other observations were made along line R, from the southern tip of the Queen Charlotte Islands out to station Papa. Both lines are in the southern area of the Gulf of Alaska where satellite data (Figure 2) and earlier ship data (Figure 6) indicate that eddy activity is relatively low.

Figure 7 shows the time series of geopotential anomalies interpolated from data collected on 12 cruises along line P in the years 1986-1989. The largest observed anomaly, with a height of 10cm, was observed at a single (but duplicated) station on the June/July 1988 cruise and was not observed on the May or November 1988 cruises.

Figure 8 shows data for these two cruises compared with the sequence of satellite data interpolated along line P. The heavy lines show ship measurements from the two cruises with the mean slope removed. The May data show no anomaly higher than about 3cm, the June data show the 10cm anomaly in duplicated measurements at station P18. The dotted lines show the sequence of Geosat height measurements from October 1987 (top) to October 1988 (bottom). The mean dates for some of the satellite cycles are indicated by the arrows, and the ship data is plotted over the corresponding satellite data.

On the June cruise the eddy gave a 10cm amplitude at one station and amplitudes less than 3cm at adjacent stations, 40nm (72km). Geosat tracks cross line P at intervals of about 60nm (105km) and give amplitudes of about 5cm on each side of the peak.

This observation confirms that the Geosat tracks are spaced too widely for optimum detection of height anomalies. The low anomaly amplitude observed in both ship and satellite data lead to an estimated 5cm detection limit for these eddies with the present satellite data. The precision of the ship data is estimated (from repeat observations) as about 1cm.

5 GEOSAT OBSERVATIONS OF SURFACE WAVEHEIGHT.

An essential step in deriving a precise range from Geosat altimeter data is the fitting of the observed shape of the leading edge of the return signal, averaged over many pulses, to the expected shape for different values of satellite attitude, wind speed and significant wave height (Hayne and Hancock, 1990). The resulting estimates of waveheight are immune from many sources of error, since they depend only on the shape of the pulse and are independent of the received signal strength, which varies with atmospheric and ionospheric attenuation, and with surface reflectance, and of propagation delays. For an instrument such as that launched on Geosat, the narrow pulse width easily resolves waveheight changes of 0.5m in $H_{1/3}$ (significant wave height or 4 standard deviations of the measured height distribution).

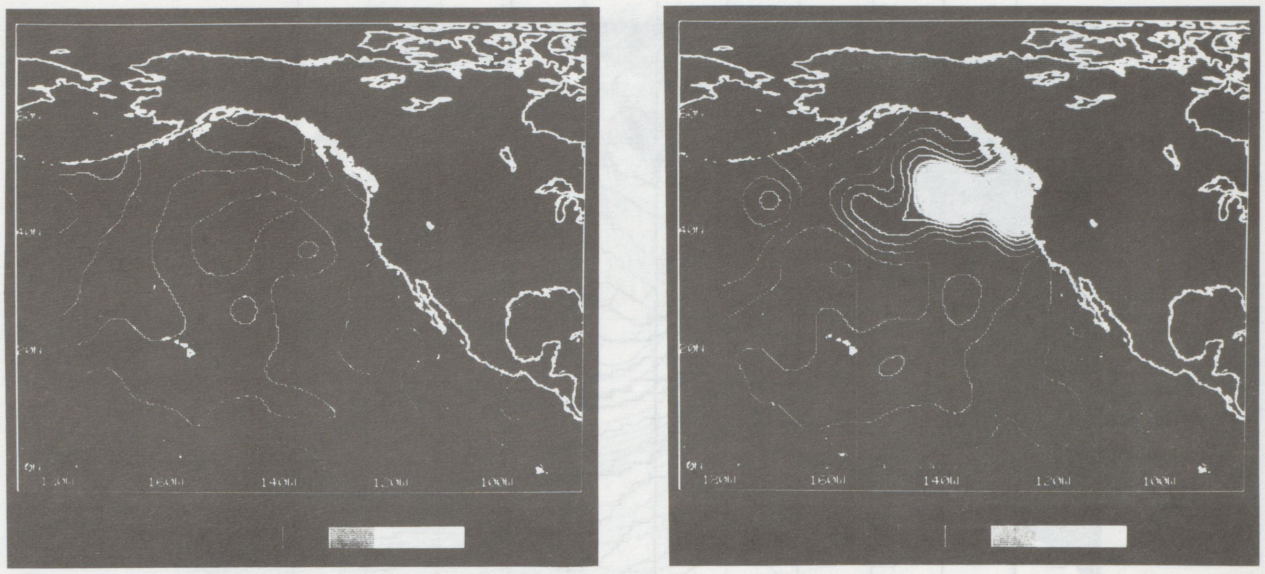

Figure 9. Grey scale 3-day composite images of waveheight in the north-east Pacific showing calm areas dark and rough areas light. Height contours of half meter intervals in $H_{1/3}$ are shown as heavy lines. Left, Figure 9a: composite image for November 14-16, 1987. Right, Figure 9b: composite image for November 17-19, 1987.

The quasi-random distribution of sea surface heights limits the precision of all waveheight measurements. Increased precision is only achievable by increased averaging, either in space or in time. The standard 20 minutes of single point data from a wave-rider buoy is equivalent to about 100 wave periods, of 10 second, 156m waves, giving about a 10% accuracy in waveheight. For the satellite, the shape of a single radar altimeter pulse is affected by the speckle noise in the coherent microwave data. Geosat data is averaged over 1 second, during which time the altimeter transmits and receives 1000 pulses. The average pulse shape should therefore be stable to about 3%.

The leading-edge shape of an individual pulse return is determined by the average wave field over a circle centered on the nadir point directly beneath the satellite. The radius of the circle increases from about 2km for a calm sea to 8km for waves with $H_{1/3}$ = 10 meters. If sea surface heights are considered to be coherent over an area equal to about the square of the peak energy wavelength, then for 156m waves there would be about 2000 independent samples over a 4km radius circle, giving over an order of magnitude more averaging than from a wave-rider. In one second the satellite nadir point will have moved about 6.5km, so that the next 1 second average covers a nearly independent area.

In their amount of averaging, the waveheight measurements from a satellite altimeter are superior to those collected by surface buoy measurements. However, there is no exact and accepted standard against which both techniques can be compared. Certainly satellite results show high self-consistency, and agreement with the buoy results is within satellite specifications (Dobson et al., 1987, Monaldo, 1988). The nature of the ocean wave/radar interaction may introduce systematic errors in the satellite measurements.

The sampling areas of the altimeter waveheight measurements are very small compared to the distance between tracks on a given day. Effectively, the measurements are made only along the satellite's track, and the coverage from a single satellite severely limits the accuracy of maps compiled by interpolating between the tracks.

A much more frequent coverage than the 17 day repeat cycle is needed to avoid aliasing of varying or moving storms over the repeat period. In a single day, satellite tracks are spaced about 3000km apart at the equator, or 2000km at 45^{o}N. In 3 days the Geosat orbit has an approximate repeat pattern in which these separations are reduced to about 1000km (700km at 45^{o}N). Ascending and descending passes combine to diagonal grids of tracks of this spacing.

Three days is longer than optimum, and 1000km is also too large in the spatial domain, so the coverage from a single satellite is again inadequate. However, for the examples that follow, the 3 day pattern is used as the best compromise.

Figure 9 shows two waveheight maps of the north-east Pacific compiled from consecutive 3 day sequences of data. Positions of the satellite tracks from which data are used, are shown. Data is interpolated to fill the entire area using a gaussian weighting of data with distance as in Figures 3 and 4, but with an e-folding distance of 800km.

In Figure 9a the ocean is relatively calm, with the highest waveheight contour being 3.5m, and the lowest 1.5. In Figure 9b an intense storm is centered in the Gulf of Alaska. Peak observed waveheights were over 10m, but the smoothing of the 3 day composite reduces this to 7.7m. The highest contour is 7.5m, the lowest 1.5, as before.

The shape and data values in the high wave area are strongly affected by the positions of the tracks from which data is combined. However statistical, wave climate, information will not be degraded. Figure 10 shows an image of the average waveheight for the period November 8 to December 22 1987. This clearly shows the band of high waveheights along 45^{o}N (highest contour is 4m) and the decrease towards the south and southwest (lowest contour is 1.5m). Figure 10b shows the standard deviation associated with this average. The figure shows two regions where the range of measured waveheights is high, one centered at 47^{o}N and 137^{o}W, close to the storm centre in Figure 9b, and the other further west, near 180^{o}W.

Longer data series are needed to show seasonal and interannual variations. For many regions of the world Geosat data will provide the most accurate wave climate data available. Even in areas well served by conventional observations, the consistency, high accuracy and wide spatial and temporal coverage from the satellite will give a great improvement in quality of data.

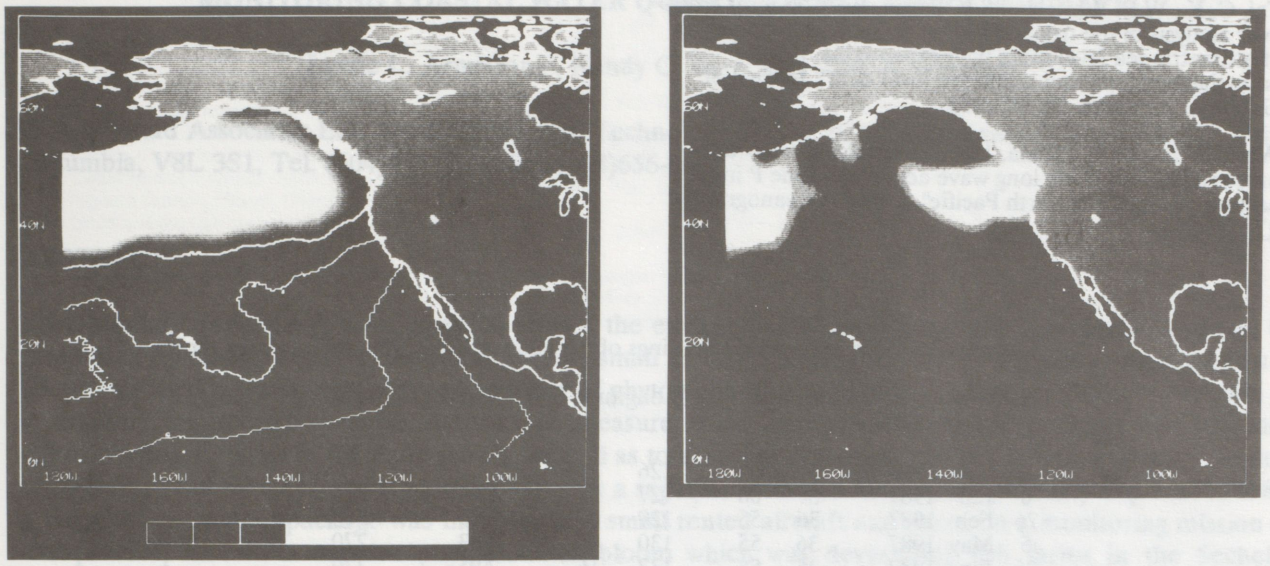

Figure 10. Grey scale images of average and standard deviations of the 3-day composite waveheight maps similar to those in Figure 9 for the north-east Pacific. Left, Figure 10a: average for the period November 8 1986 to December 22 1986. Right, Figure 10b: standard deviation, or effectively, height range for this period.

6 CONCLUSIONS

Geosat altimetry is providing the first convincing and detailed data on Rossby wave-like features. The resulting information on eddy formation and movement can considerably expand our knowledge of ocean dynamics.

The magnitudes and distribution of the anomalies agree well with the available ship observations. The slopes measured near major height anomalies are of order 30cm over 100km, implying geostrophic currents of about 25cm/s. Such currents may play a significant role in the event of a major oil spill, and satellite altimetry could then be an important source of accurate and timely data for predicting oil dispersal.

Both satellite and ship observations find that isolated eddies tend to be anti-cyclonic in the Gulf of Alaska. The strongest eddy observed off California is cyclonic with a negative height anomaly of 20-30cm.

The comparison with ship data shows that eddies can be small enough to be undersampled with the Geosat tracks. The limiting sensitivity for eddy location appears to be about 5cm.

The waveheight data presented also shows the limitation of coverage from a single satellite for operational waveheight mapping. However, the wave climate data available from Geosat should find important applications in ocean system design and planning and in a variety of scientific studies, including climate research.

The value of a sequence of satellite data increases with the length of the time period covered. Geosat ceased to operate in mid 1989. We look forward to launch of a replacement system as soon as possible.

7 ACKNOWLEDGEMENTS

Funding from the Radar Data Development Program administered by the Department of Energy, Mines and Resources, and help with the analysis from Maria del Mar Martinez de Saavedra Alvarez, are gratefully acknowledged.

8 REFERENCES

Cheney, R.E., J.G. Marsh and B.D. Beckley, 1983, "Global mesoscale variability from co-linear tracks of SEASAT altimeter data" Journal of Geophys. Research, 88, 4343-4354.

Dobson, B, F.M. Monaldo, J. Goldhirsh and J. Wilkerson, 1987, "Validation of Geosat altimeter-derived wind speeds and significant wave heights using buoy data", Journal of Geophys. Research, 92, 10719-10731.

Douglas, B.C. and R.E. Cheney, 1990, "Geosat: beginning a new era in satellite oceanography", Journal of Geophys. Research, 95, 2833-2836.

Fu, L.-L., and D.B. Chelton, 1985, "Observing large-scale temporal variability of ocean currents by satellite altimetry: with reference to the Antarctic Circumpolar Current", Journal of Geophys. Research, 90, 4721-4739.

Gower, J.F.R., 1989a, "Sea surface height anomalies in the north-east Pacific: the Sitka eddy", Proceedings of IGARSS'89/12th Canadian Symposium on Remote Sensing, July 10-14, Vancouver, B.C., IEEE Publ 89CH2780-0, Vol 2, pp.1059-1062.

Gower, J.F.R., 1989b, "Geosat altimeter observations of the distribution and movement of sea-surface height anomalies in the north-east Pacific", Proceedings of OCEANS'89, Sept 18-21, Seattle, Washington, USA, IEEE Publ 89CH2780-5, Vol 3, pp.977-981.

Hayne, G.S. and D.W. Hancock III, 1990, "Corrections for the effects of significant wave height and attitude on Geosat radar altimeter measurements", Journal of Geophys. Research, 95, 2837-2842.

Monaldo, F.M., 1988, "Expected differences between buoy and radar estimates of wind speed and significant wave height and their implications on buoy-altimeter comparisons", Journal of Geophys. Research, 93, 2285-2302.

Tabata, S. 1982 "The anticyclonic, baroclinic eddy off Sitka, Alaska, in the northeast Pacific Ocean" Journal of Physical Oceanography, 12, 1260-1282.

Tai, C.-K., W.B. White and S.E. Pazan, 1989, "Geosat cross-over analysis in the tropical Pacific. 2. Verification analysis of altimetric sea level maps with expendable bathythermograph and island sea level data", Journal of Geophys. Research, 94, 897-908.

White W.B. and S. Tabata, 1987, "Interannual westward-propagating baroclinic long wave activity on Line P in the eastern mid-latitude north Pacific", J. Phys. Oceanography, 17, 385-396.

Table 1: Positions, speeds and headings of the eddy off California on the dates shown.

Mean date	Latitude	Longitude	Speed (cm/s)	Heading (E from N)
17 Nov 1986	37 06	126 23		
6 Jan 1987	37 06	127 51	2.95	270
26 Feb 1987	36 55	129 07	2.57	260
5 May 1987	36 55	130 48	2.53	270
25 Jun 1987	36 55	132 16	2.95	270
15 Aug 1987	36 55	133 20	2.03	270

Table 2: Positions, displacements, speeds and headings of the eddies whose tracks are plotted in Figure 5, deduced from positions at the cycle numbers indicated.

Eddy	Cycle	Lat.	Long.	Km	Days	cm/s	Heading
A	6	59 15	-141 25				
	13	58 34	-143 21	135.22	119.3	1.31	236.30
	19	58 40	-145 18	113.99	102.3	1.29	275.53
	34	57 13	-149 27	173.04	136.4	1.47	236.64
S	12	57 34	-138 52				
	17	57 38	-141 17	144.71	85.2	1.96	272.90
	23	57 13	-142 54	106.96	102.3	1.21	244.68
B	3	54 21	-134 44				
	9	54 41	-136 42	132.10	102.3	1.49	286.09
	15	54 35	-139 11	160.65	102.3	1.82	266.08
	23	55 9	-140 27	101.17	136.4	0.86	307.95
	34	54 52	-141 22	66.84	187.5	0.41	242.26
C	1	55 58	-142 26				
	4	55 34	-142 54	52.85	51.1	1.20	213.79
	8	55 18	-144 0	75.21	68.2	1.28	247.09
	13	54 7	-145 15	152.94	85.2	2.08	211.84
H	7	51 57	-132 6				
	13	51 33	-133 18	93.83	102.3	1.06	242.09
	19	51 36	-134 52	108.39	102.3	1.23	272.90
	27	51 58	-136 53	145.05	136.4	1.23	286.11
	34	51 21	-137 36	83.89	119.3	0.81	216.18